Key Points:
- The mechanisms driving interannual variation in oxygen isotopes in Amazon tree rings ($\delta^{18}O_{TR}$) have previously not been fully understood
- We show that Amazon basin-intrinsic processes control interannual variation in $\delta^{18}O_{TR}$, with upstream rainout the most important factor
- Our results show that $\delta^{18}O_{TR}$ can be reliably used to reconstruct Amazon precipitation, with wider implications for other $\delta^{18}O$ proxy records

Supporting Information:
- Supporting Information S1

Correspondence to:
J. C. A. Baker,
gyjcab@leeds.ac.uk

What drives interannual variation in tree ring oxygen isotopes in the Amazon?

J. C. A. Baker[1], M. Gloor[1], D. V. Spracklen[2], S. R. Arnold[2], J. C. Tindall[2], S. J. Clerici[1], M. J. Leng[3,4], and R. J. W. Brienen[1]

[1]School of Geography, University of Leeds, Leeds, UK, [2]School of Earth and Environment, University of Leeds, Leeds, UK, [3]NERC Isotope Geosciences Facilities, British Geological Survey, Nottingham, UK, [4]Centre for Environmental Geochemistry, University of Nottingham, Nottingham, UK

Abstract Oxygen isotope ratios in tree rings ($\delta^{18}O_{TR}$) from northern Bolivia record local precipitation $\delta^{18}O$ and correlate strongly with Amazon basin-wide rainfall. While this is encouraging evidence that $\delta^{18}O_{TR}$ can be used for paleoclimate reconstructions, it remains unclear whether variation in $\delta^{18}O_{TR}$ is truly driven by within-basin processes, thus recording Amazon climate directly, or if the isotope signal may already be imprinted on incoming vapor, perhaps reflecting a pan-tropical climate signal. We use atmospheric back trajectories combined with satellite observations of precipitation, together with water vapor transport analysis to show that $\delta^{18}O_{TR}$ in Bolivia are indeed controlled by basin-intrinsic processes, with rainout over the basin the most important factor. Furthermore, interannual variation in basin-wide precipitation and atmospheric circulation are both shown to affect $\delta^{18}O_{TR}$. These findings suggest $\delta^{18}O_{TR}$ can be reliably used to reconstruct Amazon precipitation and have implications for the interpretation of other paleoproxy records from the Amazon basin.

1. Introduction

Relationships between oxygen isotopes ($\delta^{18}O$) and environmental variables have often been the basis for paleoclimate reconstructions, but relying on empirical correlations alone without an understanding of the underlying mechanisms may lead to misinterpretations of proxy records [*McCarroll and Loader*, 2004]. In the Amazon, $\delta^{18}O$ in paleoarchives (including speleothems, lake and marine sediments, and ice cores [e.g., *Kanner et al.*, 2013; *Maslin and Burns*, 2000; *Moquet et al.*, 2016; *Thompson et al.*, 2013; *Vuille et al.*, 2012, and references therein] offer valuable insights for climate in the absence of quality instrumental data. In addition to these, $\delta^{18}O$ in annual tree rings ($\delta^{18}O_{TR}$) have been identified as a useful tool for precipitation reconstructions [*Baker et al.*, 2015; *Ballantyne et al.*, 2011; *Brienen et al.*, 2012]. The $\delta^{18}O_{TR}$ reflect soil water $\delta^{18}O$, modified, to a greater or lesser extent, by plant physiological influences, including leaf-water enrichment at the site of evaporation, back-diffusion of this enriched water to the rest of the leaf (the Péclet effect), and biological fractionation during metabolic processes [*Barbour et al.*, 2004; *Roden et al.*, 2000]. Local climate can affect plant physiology, and thus $\delta^{18}O_{TR}$ [*Kahmen et al.*, 2011], although *Brienen et al.* [2012] found that $\delta^{18}O_{TR}$ from the warm, humid rainforest of northern Bolivia recorded local precipitation $\delta^{18}O$ ($\delta^{18}O_P$), with limited evidence of a local climate influence, possibly because leaf-water isotopic enrichment is low when relative humidity is high [*Cernusak et al.*, 2016]. Instead, $\delta^{18}O_{TR}$ were found to correlate with precipitation over the whole Amazon basin during the last century [*Brienen et al.*, 2012]. The authors hypothesize that this relationship is driven by rainout of heavy isotopes during moisture transport over the Amazon basin, although $\delta^{18}O_{TR}$ were also found to correlate with the El Niño–Southern Oscillation (ENSO), possibly indicating an alternative proximal driver of interannual variation. Similar relationships with ENSO have been reported for $\delta^{18}O_{TR}$ records elsewhere in the tropics, including Ecuador [*Volland et al.*, 2016], Central America [*Anchukaitis and Evans*, 2010], northern Australia [*Boysen et al.*, 2014], and several sites in Southeast Asia [*Poussart et al.*, 2004; *Sano et al.*, 2012; *Schollaen et al.*, 2014; *Xu et al.*, 2011, 2013, 2015]. This leaves some doubt over the extent to which interannual variation in $\delta^{18}O_{TR}$ in Bolivia is driven by processes within the Amazon basin or is more representative of processes occurring at the pan-tropical scale. This is important to clarify if such isotope data are to be reliably used to reconstruct climate and potentially validate output from general circulation models (GCMs) in the Amazon [*Henderson-Sellers et al.*, 2002].

Contrasting interpretations of $\delta^{18}O$ in Andean ice cores ($\delta^{18}O_{ICE}$) suggest that the drivers of variation in $\delta^{18}O_P$ in the Amazon region are still not fully understood. It has been proposed that tropical ice cores record

changes in temperature, as they do at higher latitudes [*Thompson et al.*, 1995, 2000, 2006], but analyses using Rayleigh fractionation models instead suggest that ice cores primarily reflect changes in regional hydrology [*Grootes et al.*, 1989; *Hoffmann*, 2003b; *Pierrehumbert*, 1999; *Samuels-Crow et al.*, 2014]. Rayleigh models predict the depletion of water vapor isotopes during moisture transport across the Amazon basin as heavy isotopes are preferentially removed during precipitation events [*Dansgaard*, 1964; *Salati et al.*, 1979]. A recent Rayleigh-based model including the influence of South American cold-air incursions (typically associated with positive precipitation anomalies in the western Amazon basin [*Hurley et al.*, 2015]) was able to simulate ~74% of the daily variability in Andean snowfall $\delta^{18}O$ [*Hurley et al.*, 2016]. However, studies have also shown that Rayleigh models could be an oversimplification in tropical South America, not least due to large-scale water recycling by vegetation [*Brown et al.*, 2008; *Salati et al.*, 1979; *Sturm et al.*, 2007]. This is because transpiration at steady state is a nonfractionating process, which returns heavy isotopes to the atmosphere and accounts for the weak continental gradient in $\delta^{18}O_P$ over the Amazon [*Insel et al.*, 2013; *Salati et al.*, 1979]. Transpiration therefore needs to be considered in an assessment of the controls on Amazon $\delta^{18}O_P$.

Several recent studies have used trajectory modeling as a tool to develop a better understanding of Amazon water vapor transport. Trajectory analysis can be used to identify moisture origins and detect changes in atmospheric transport/circulation that might influence $\delta^{18}O_P$ [*Drumond et al.*, 2014; *Fiorella et al.*, 2015; *Insel et al.*, 2013; *Spracklen et al.*, 2012; *van der Ent et al.*, 2010]. Trajectories have also been used in conjunction with GCMs [*Sturm et al.*, 2007] and satellite isotope data [*Brown et al.*, 2008] to track isotope changes during atmospheric transport. Furthermore, transport analysis has previously been used to identify climate controls on water isotopes in precipitation in the western Amazon [*Villacís et al.*, 2008; *Vimeux et al.*, 2005]. In both of these studies upstream rainout was identified as the most important factor in determining the isotopic composition of precipitation, with local environmental variables having little or no effect on the signal. However, these studies, which spanned 5 years and 22 months, respectively, specifically looked at controls on seasonal isotope variability and were too short to thoroughly investigate controls on isotope variation at interannual time scales.

Here we aim to resolve the ambiguity surrounding the interpretation of tree ring $\delta^{18}O$ records from the Amazon, and thus strengthen the use of these, and other $\delta^{18}O$ proxy records, in paleoclimate reconstructions and for possible use in validating climate models. Existing records of $\delta^{18}O_P$ in the region (e.g., in the Global Network of Isotopes in Precipitation database) are often short and discontinuous, preventing a detailed assessment of climate controls at interannual time scales. The $\delta^{18}O_{TR}$ record that we use here is continuous and annual and can therefore be calibrated against modern climate data and used to identify mechanisms driving interannual variability. To achieve this we use air mass back trajectories combined with satellite observations of precipitation and leaf area index (LAI), which is a good proxy for evapotranspiration in the tropics [*Spracklen et al.*, 2012], and fields from the ERA-Interim reanalysis (which combines model data with observations) to investigate the causal drivers of interannual variation in $\delta^{18}O_{TR}$ over a 32 year period.

2. Data and Methodology

This study uses a $\delta^{18}O_{TR}$ chronology developed from nine trees from Selva Negra, Bolivia (10°5′S, 66°18′W; 160 m above sea level), which has been shown to record local precipitation $\delta^{18}O$ [see *Baker et al.*, 2015; *Brienen et al.*, 2012]. We used two approaches to identify the influence of Amazon basin processes on the observed $\delta^{18}O_{TR}$ signal: (1) trajectory modeling to reconstruct air mass histories and (2) large-scale water vapor transport analysis.

To assess the relationship between $\delta^{18}O_{TR}$ and air mass history we used a Lagrangian atmospheric transport model to calculate kinematic back trajectories. ERA-Interim reanalysis wind fields were retrieved from the European Centre for Medium-Range Weather Forecasts (http://www.ecmwf.int/en/research/climate-reanalysis/era-interim) to drive the model, with trajectory position output every 6 h. We calculated 10 day back trajectories arriving daily (12.00 UT) 2 km above the surface (800 hPa) at Selva Negra for the period of 1998–2011. This height is likely to be within the bounds of low-level moisture advection and close to the height of precipitation onset [*Andreae et al.*, 2004]. There are uncertainties associated with trajectories as they are inherently simplistic, and may struggle to capture all of the complexities of tropical atmospheric circulation, particularly subgrid-scale convective transport processes [*Stohl*, 1998]. Here we use three-dimensional trajectories which have been shown to be more accurate than other calculation methods [*Stohl and*

Seibert, 1998]. Altitude sensitivity analysis confirms our results to be robust within 1–4 km above the surface (Figure S2 in the supporting information).

Trajectories were used to reconstruct air mass histories, including precipitation and exposure to vegetation. Precipitation data come from the Tropical Rainfall Measuring Mission (TRMM) 3B42 v7 product, which combines data from TRMM and other satellites [*Huffman et al.*, 2007]. We summed precipitation along each back trajectory for 10 days or until it reached the coast (whichever of these came first). This was done by accumulating precipitation at the trajectory latitude (lat) and longitude (lon) for every 6 h time step (t) and then averaging these values across a number of trajectories (n) to find mean accumulated precipitation (ΣPrecip), according to the equation: $\sum_{t=0}^{-40} \text{Precip}\,(\text{lat}_n\,(t), \text{lon}_n\,(t))\Delta(t)$. Trajectories were averaged across different time periods (3 months, wet season (October–April) and dry season (May–September)) to extract the relative influence of $\sum$Precip on $\delta^{18}O_{TR}$ for different periods of the year. The analysis was limited to those trajectories arriving on days with rain >0 mm at Selva Negra, as these are the air mass histories that contribute to the $\delta^{18}O_{TR}$ signal. LAI data from the Moderate Resolution Imaging Spectroradiometer [*Myneni et al.*, 2002] were used to calculate accumulated LAI ($\sum$LAI) using the same methodology. The influences of other climatic variables, including temperature, were also analyzed (see Method S1 in the supporting information).

In our second approach we used ERA-Interim data to conduct an analysis of large-scale moisture transport into and out of the Amazon basin. Wind fields from 0 to 4 km above the surface were averaged and used to identify the dominant atmospheric transport patterns for the wet season (October–April) and define basin inflow and basin outflow transects (Figure 3a). Column-integrated northward and eastward water vapor fluxes were used to estimate average wet season moisture flow across these transects for the period of 1979–2010/2011. Wind and moisture transport anomalies were calculated for years with high and low $\delta^{18}O_{TR}$ values to qualitatively characterize differences in circulation. A more detailed discussion of the methodology can be found in the supporting information [*Bruijnzeel et al.*, 2011; *Callède et al.*, 2008; *Huffman*, 1997; *LeGrande and Schmidt*, 2006; *Majoube*, 1971; *Samanta et al.*, 2011; *Smith et al.*, 2006; *Sternberg*, 2009; *Sternberg and DeNiro*, 1983; *Yan et al.*, 2016].

3. Results

The mean climatology for our tree ring sampling site, Selva Negra, is shown in Figure 1a, based on data from the Climatic Research Unit. Temperature is fairly constant throughout the year but precipitation is highly seasonal, and there is a distinct dry season (precipitation <100 mm month^{-1}) from May to September. The tree species used to construct the $\delta^{18}O_{TR}$ chronology (*Cedrela odorata*) grows primarily during the wet season, with growth usually beginning in September/October and ending in April/May [*Brienen and Zuidema*, 2005; *Dünisch et al.*, 2003]. Air mass histories from this period are therefore likely to have most influence on $\delta^{18}O_{TR}$. Seasonal variation in $\delta^{18}O_P$ is also shown in Figure 1. The lowest values are reached toward the end of the wet season, with a 2 month lag between peak rainfall and minimum $\delta^{18}O_P$. The highest $\delta^{18}O_P$ values are in the driest months, sometimes exceeding 0‰. Atmospheric transport is predominantly from the north and northwest during the wet season (Figure 1b), while dry season trajectories are more easterly.

A 3 month moving window correlation analysis between interannual precipitation and interannual $\delta^{18}O_{TR}$ reveals significant relationships between $\sum$Precip and $\delta^{18}O_{TR}$ throughout the wet season months, coinciding with the main growing period of *C. odorata* (Figure 2a). Correlations are consistently negative, so larger upstream precipitation corresponds with smaller $\delta^{18}O_{TR}$ values and vice versa. The strongest 3 month correlation occurs in November–January ($r = -0.84$, $p < 0.001$; 1998–2010/2011) when precipitation is reaching its annual peak (Figure 1a). When trajectories from the dry and wet seasons are considered separately only $\sum$Precip$_{WET}$ is significantly related to $\delta^{18}O_{TR}$. This close relationship is shown in Figure 2b. Although the time series is relatively short (13 years) the relationship is highly significant ($r = -0.85$, $p < 0.001$) with $>70\%$ of the interannual variation in $\delta^{18}O_{TR}$ explained by ΣPrecip$_{WET}$. This provides a clear indication that the mechanism driving variation in $\delta^{18}O_{TR}$ on interannual time scales is rainout during moisture transport over the Amazon basin.

To determine whether the correlation between $\delta^{18}O_{TR}$ and ΣPrecip$_{WET}$ is driven by interannual variation in the position and speed of the transport pathway or interannual variation in the precipitation amount over
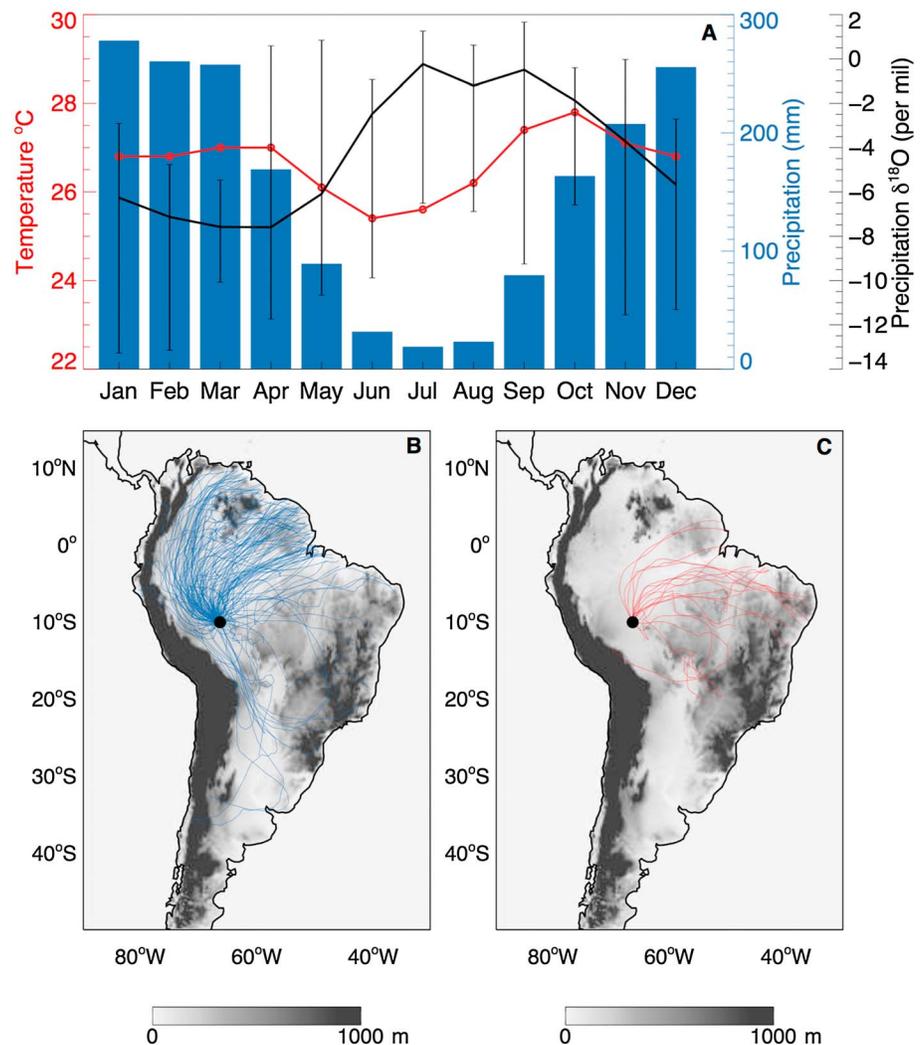
Figure 1. (a) Climate diagram for Selva Negra, Bolivia (10°5′S, 66°18′W). Temperature and precipitation data are from 65–67.5°W, 9–11.5°S CRU TS3.21, 1960–2010. Monthly $\delta^{18}O_P$ data are averaged from four stations in the GNIP database. The error bars represent the maximum and minimum observations in each month across all sites. (b) Daily trajectories arriving at 800 hPa on days with precipitation >0 mm at Selva Negra (black circle) during the 2010/2011 wet season (October–April). (c) Same as in Figure 1b but for the 2010 dry season (May–September). Trajectories are plotted over a topographical map of South America (Shuttle Radar Topographic Mission data).

the basin we conducted two sensitivity experiments where we systematically controlled for variation in precipitation and trajectory position in the calculation of $\sum Precip_{WET}$. Experiment 1 used climatological precipitation (i.e., not interannually varying) from the observed trajectories, and experiment 2 used observed precipitation data from trajectory paths kept constant from year to year (see Method S1). Significant relationships between $\sum Precip_{WET}$ and $\delta^{18}O_{TR}$ were found in both of these experimental scenarios, suggesting that interannual variation in Amazon basin precipitation and variation in atmospheric circulation are both important in driving the relationship (Table S1 in the supporting information).

The effects of other air mass history attributes on $\delta^{18}O_{TR}$ were also investigated. A positive relationship between $\delta^{18}O_{TR}$ and $\sum LAI$ (which is directly associated with evapotranspiration [see *Spracklen et al.*, 2012]) was anticipated since evaporative recycling might be expected to return isotopically heavy water back to the atmosphere and thus reduce continental rainout [*Salati et al.*, 1979]. In fact, $\delta^{18}O_{TR}$ and $\sum LAI$ were found to anticorrelate during the wet season (Figure S1). This may be due to the positive correlation between $\sum LAI$ and $\sum Precip$ across all wet season trajectories from 2000 to 2011 ($r = 0.31$, $p < 0.001$, $n = 1981$). Further analysis showed that $\sum LAI$ also correlated strongly with trajectory time spent over land ($r = 0.82$, $p < 0.001$,
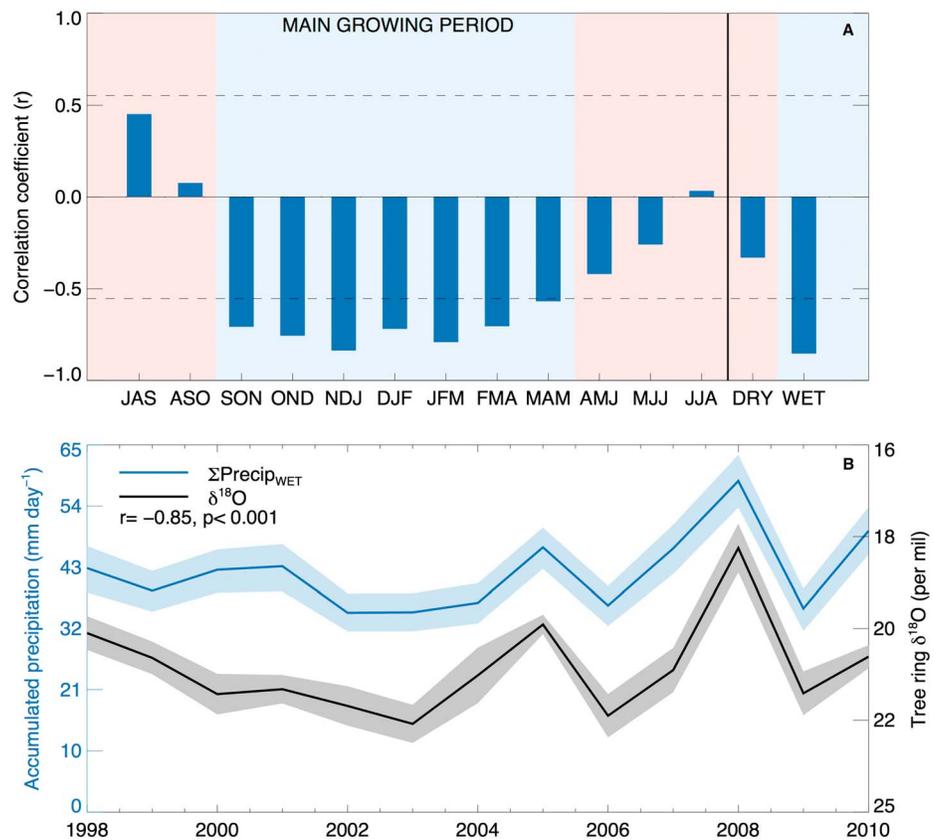
Figure 2. (a) Three-month moving correlation coefficients between $\delta^{18}O_{TR}$ and mean accumulated TRMM precipitation ($\sum$Precip; trajectories from 1998 to 2010/2011). The pink and blue boxes show the dry and wet seasons, respectively. The bars at the right side of the plot show the mean correlation coefficients for the dry season (May–September) and wet season (October–April). The broken horizontal lines mark the significance threshold ($p < 0.05$). (b) Interannual variation in $\sum$Precip$_{WET}$ and $\delta^{18}O_{TR}$ from 1998 to 2010. The shading indicates the 95% confidence intervals. Pearson's r is -0.85 ($p < 0.001$). Note that the scale for $\delta^{18}O_{TR}$ has been reversed.

$n = 1981$); thus, the relationship between $\sum$LAI and $\delta^{18}O_{TR}$ arises because $\sum$LAI is a proxy for travel time, and longer times provide more opportunity for fractionation processes such as rainout to occur. The effects can be teased apart by controlling for the effect of $\sum$Precip on $\delta^{18}O_{TR}$ and $\sum$LAI, resulting in mostly nonsignificant relationships between $\sum$LAI and $\delta^{18}O_{TR}$ (Figure S1). We also looked at the influence of temperature during atmospheric transport. Temperature data were from ERA-Interim and specific to the horizontal and vertical positions at each trajectory time step. Mean back trajectory temperature was found to have no significant relationship with $\delta^{18}O_{TR}$.

To complement the analysis above, and to overcome the limitations of a short temporal record of remote sensing data, a basin-scale analysis of water vapor transport was carried out using ERA-Interim reanalysis data from 1979 to 2011 (Figures 3, S5, and S6). Figure 3d shows a strong negative relationship between net wet season moisture balance (water vapor inflow-water vapor outflow) and both Selva Negra $\delta^{18}O_{TR}$ ($r = -0.76$, $p < 0.001$, $n = 32$) and the $\delta^{18}O_{TR}$ record from *Brienen et al.* [2012] ($r = -0.73$, $p < 0.001$, $n = 23$). The difference between water vapor inflow and outflow should be approximately equal to net rainout and indeed correlates strongly with Amazon annual river discharge measured at Óbidos ($r = 0.80$, $p < 0.001$, $n = 32$; Figure S4). These results further support the idea that tree rings from the southern Amazon capture large-scale patterns of precipitation and moisture recycling. When inflow and outflow are considered separately it becomes clear that the relationship between $\delta^{18}O_{TR}$ and basin moisture balance is entirely driven by variation in the amount of outflowing water vapor as $\delta^{18}O_{TR}$ correlates strongly with moisture outflow and only weakly with inflow ($r = 0.80$, $p < 0.001$ versus $r = -0.35$, $p < 0.05$; Selva Negra record). This is consistent with the results from our trajectory analysis, since variation in outflow will be directly affected by variation in rainout over the basin.
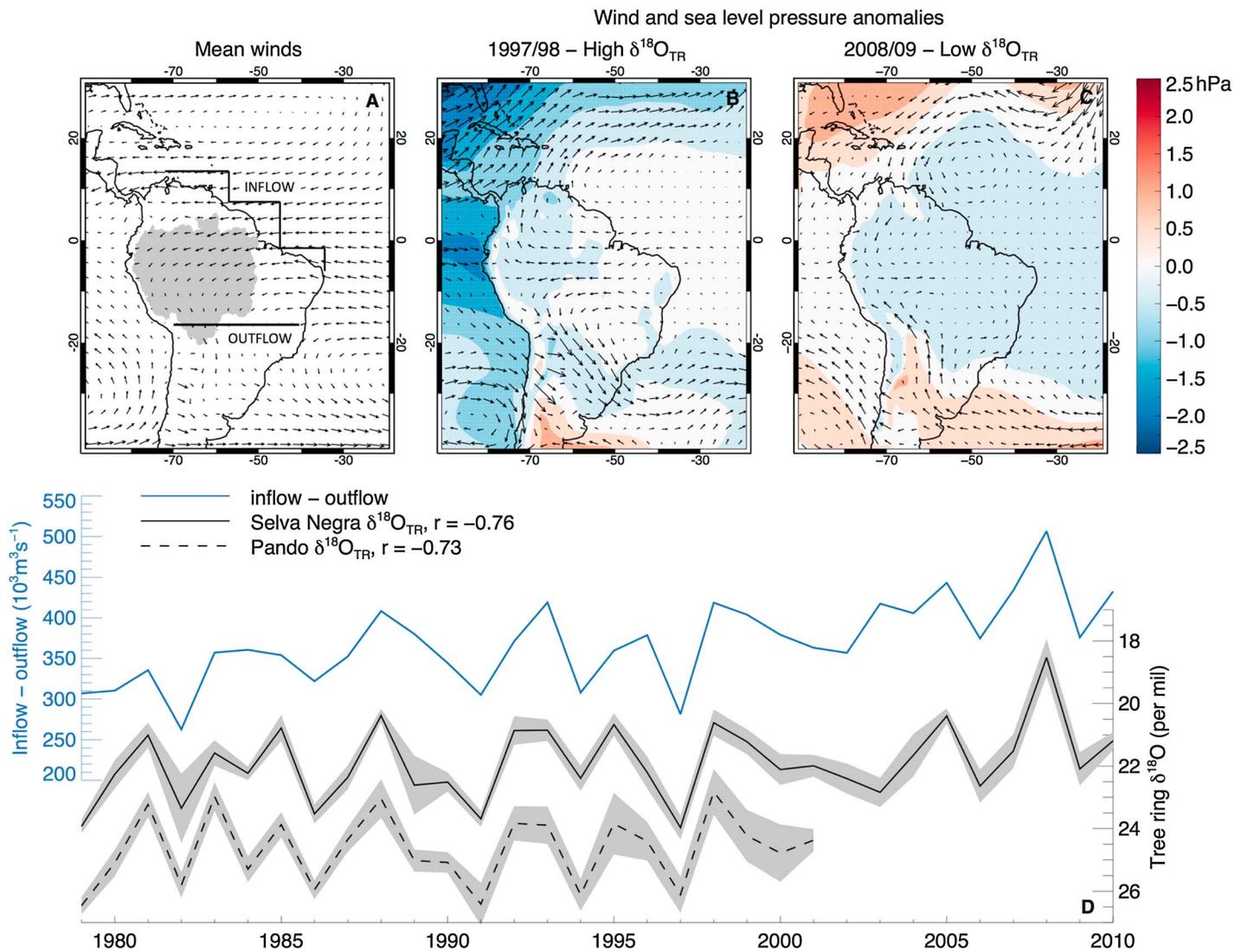
Figure 3. (a) Map of mean wet season (October–April, 1979–2010/2011) wind vectors 0–4 km above the surface and the transects used to calculate water vapor inflow to, and outflow from, the Amazon basin (shaded in grey). (b) Map of wet season wind and sea level pressure anomalies in 1997/1998 (a high $\delta^{18}O_{TR}$ year). (c) Same as in Figure 3b but for 2008/2009 (a low $\delta^{18}O_{TR}$ year). (d) Interannual variation in net wet season water vapor import (inflow-outflow) and $\delta^{18}O_{TR}$ from two sites in northern Bolivia (see *Baker et al.* [2015] for a detailed comparison of these records). The shading indicates the 95% confidence intervals. Correlation coefficients between $\delta^{18}O_{TR}$ and inflow-outflow are given ($p < 0.001$). Note that the scale for $\delta^{18}O_{TR}$ has been reversed. All climate data are from the ERA-Interim reanalysis.

Compared with the variation in the outflow, moisture inflow shows relatively low interannual variation (5.8 versus 14.7%), which may further explain why $\delta^{18}O_{TR}$ correlates poorly with inflow. These findings confirm that convection and moisture removal over the basin drive interannual variability in $\delta^{18}O_{TR}$.

4. Discussion

Amazon climate is characterized by highly seasonal precipitation, with moisture transported in from the tropical Atlantic and then moving westward and southward over the basin (Figures 1, 3a, and S3). The significant anticorrelations between $\delta^{18}O_{TR}$ and $\sum Precip_{WET}$ (Figure 2b), and between $\delta^{18}O_{TR}$ and basin moisture balance (Figure 3d), demonstrate a clear link between the amount of moisture removed from the atmosphere during transport across the basin and isotopic variability. The analysis provides a mechanistic link to explain why tree rings at the far end of the Amazon basin can record precipitation over a region approximately 6 M km² [*Brienen et al.*, 2012]. The preferential removal of heavy isotopes during each precipitation event during

moisture transport depletes the water vapor remaining in the atmosphere according to the Rayleigh model [*Dansgaard*, 1964], and thus, years with more rainout correspond with more depleted values in the $\delta^{18}O_{TR}$ record. This large-scale control on the isotope signal can account for the excellent coherence between $\delta^{18}O_{TR}$ records from sites >300 km apart [*Baker et al.*, 2015]. Our results are also in agreement with studies examining the climatic drivers of isotope variability in South American precipitation on shorter time scales [*Villacís et al.*, 2008; *Vimeux et al.*, 2005]. Correlation coefficients are strongest during the wettest months (Figure 2a), which is in line with previous findings from regional circulation models [*Sturm et al.*, 2007]. It is worth observing that the severe droughts of 2005 and 2010 are not distinguishable in our isotope record as these were predominantly dry season phenomena [*Espinoza et al.*, 2011; *Marengo et al.*, 2011].

Interannual variation in basin-wide precipitation and interannual variation in transport route are both shown to be important factors affecting variation in $\delta^{18}O_{TR}$ in the Amazon (Table S1). This confirms that within-basin processes determine the isotope signal in north Bolivia. Circulation changes have been highlighted before as a potential source of variation in South American $\delta^{18}O_P$. First, variation in the contribution of moisture from isotopically distinct sources has been suggested as an important control on $\delta^{18}O_P$ at interglacial [*Cruz et al.*, 2005; *Pierrehumbert*, 1999] but also interannual [*Insel et al.*, 2013; cf. *Vuille et al.*, 2003] time scales. However, spatial variation in ocean surface $\delta^{18}O$ ($\delta^{18}O_{SW}$) in the main moisture source region for the Amazon is <1‰ (Figure S7), and thus, variation in trajectory origin is unlikely to explain much of the 4–6‰ variability in $\delta^{18}O_{TR}$. Alternatively, different transport pathways may be associated with different amounts of rainout (e.g., due to differences in topography, path length over land, and climate), and thus, interannual variation in circulation may drive interannual variation in $\delta^{18}O_P$ [*Fiorella et al.*, 2015]. Wind and moisture transport anomalies suggest that it is this second source of variability that is important at our sample site and over the time scale of our study (Figures 3, S5, and S6). Although there is substantial spatial variability in circulation between years, high $\delta^{18}O_{TR}$ years show a clear pattern of strengthened winds and enhanced moisture outflow from the southwest corner of the Amazon basin, along the path of the South American low-level jet. Conversely, in low $\delta^{18}O_{TR}$ years the anomalies are reversed, with weaker wind flow and less moisture transported out of the basin. These circulation changes in the south of the basin explain why interannual variation in outflowing moisture is strongly related to $\delta^{18}O_{TR}$. Furthermore, this analysis can explain why $\delta^{18}O_{TR}$ from Bolivia correlates strongly with ENSO [*Brienen et al.*, 2012]: during a positive (negative) ENSO phase such as 1997/1998, (2008/2009) circulation changes accelerate (decelerate) transport out of the Amazon basin, thus leading to lower (higher) basin precipitation and higher (lower) $\delta^{18}O_{TR}$ values (Figure 3). This shows how a pan-tropical climate phenomenon like ENSO influences basin-scale processes, which in turn control interannual variation in $\delta^{18}O_{TR}$. This ENSO influence on $\delta^{18}O_{TR}$ has been reported at other sites in the tropics due to ENSO's far-reaching impact on precipitation [e.g., *Anchukaitis and Evans*, 2010; *Poussart et al.*, 2004; *Sano et al.*, 2012; *Schollaen et al.*, 2014; *Volland et al.*, 2016; *Xu et al.*, 2015].

We find a negative relationship between $\delta^{18}O_{TR}$ and air mass exposure to vegetation during the wet season, driven by a positive correlation between $\sum LAI$ and $\sum Precip$. We had anticipated $\delta^{18}O_{TR}$ to positively corre-late with $\sum LAI$, which is a proxy for evapotranspiration [*Spracklen et al.*, 2012], since evapotranspiration reduces the effective rainout by returning heavy isotopes to the atmosphere. Indeed, previous studies report a low continental gradient in $\delta^{18}O_P$ over the Amazon due to large-scale water recycling offsetting the rainout of heavy isotopes [*Insel et al.*, 2013; *Salati et al.*, 1979]. However, $\sum Precip$ and $\sum LAI$ are not in fact independent: $\sum LAI$ is a function of travel time over land, which influences the degree of fractionation likely to have occurred along the trajectory. The negative correlations between $\delta^{18}O_{TR}$ and $\sum LAI$ largely disappear when controlling for the effect of $\sum Precip$, although a significant negative relationship persists during November–January (Figure S1). This result illustrates that disentangling confounding influences on $\delta^{18}O_{TR}$ can sometimes prove a challenge.

The findings in this study have implications for the interpretation of paleoproxies in the Amazon beyond $\delta^{18}O_{TR}$. Specifically, they add support to the growing evidence base that $\delta^{18}O$ recorded in, e.g., tropical ice cores and speleothems, seem to largely reflect hydroclimate variability and not temperature variability [*Grootes et al.*, 1989; *Hoffmann*, 2003a, 2003b; *Hurley et al.*, 2016; *Hurley et al.*, 2015; *Moquet et al.*, 2016; *Pierrehumbert*, 1999; *Samuels-Crow et al.*, 2014; *Vimeux et al.*, 2005], although it must be noted that the time scales of these studies vary from interglacial scales to just a few years. However, others have argued against trying to disentangle the effects of precipitation and temperature on $\delta^{18}O$ due to the strong correlation

between these variables at interannual time scales in the tropics [e.g., *Vuille et al.*, 2003]. To complete our analysis we used a simple Rayleigh-based model to simulate interannual variation in $\delta^{18}O_{TR}$ (Method S1). The Rayleigh model predicts isotopic composition as a function of the fraction (*f*) of water vapor remaining in the atmosphere. Outputs from our trajectory analysis were used to calculate *f* keeping all temperature-dependent parameters constant from year to year. Figure S8 shows the evolution of water vapor isotopes along a sample trajectory and the Rayleigh-predicted $\delta^{18}O_{TR}$ value in each year. Our simulated $\delta^{18}O_{TR}$ values match well with observations ($r = 0.91$, $p < 0.001$, 2000–2010, root-mean-square error ≈ 1.6‰) but were twice as variable (range = 8.8 versus 4.3‰). This analysis shows that the factors controlling Amazon $\delta^{18}O_{TR}$ are well understood. To some degree the same factors are likely to influence $\delta^{18}O_{ICE}$ records from the Andes, as suggested by the relationships between lowland $\delta^{18}O_{TR}$ and $\delta^{18}O_{ICE}$ from Quelccaya and Huascarán over recent times ($r = 0.77$ and 0.68, respectively [*Brienen et al.*, 2012]). A direct correlation between a composite $\delta^{18}O_{ICE}$ record and Amazon River discharge measured at Óbidos shows that Amazon precipitation can explain about 50% of the variation in $\delta^{18}O_{ICE}$ from 1950 to 1984 (Method S1). The shift of ~6‰ in $\delta^{18}O_{ICE}$ since the Last Glacial Maximum (LGM) [*Thompson et al.*, 2000] is comparable to between-year differences of <5.5‰ (e.g., 1997 versus 2008) seen within one decade of our $\delta^{18}O_{TR}$ record, which can be almost entirely explained by changes in Amazon moisture balance. It is therefore feasible that variation in Amazon hydrology could account for most of the change in $\delta^{18}O_{ICE}$ since the LGM (i.e., a decrease in rainout since the LGM causing an increase in $\delta^{18}O_{ICE}$), without needing to invoke large shifts in temperature [*Pierrehumbert*, 1999]. However, it should be noted that during the LGM $\delta^{18}O_{SW}$ would have been ~1‰ higher due to the difference in global ice volume, although spatial gradients in tropical $\delta^{18}O_{SW}$ were similar to the present day [*Holloway et al.*, 2016].

The results presented here show that basin rainout is the most important mechanism driving interannual variability in Amazon $\delta^{18}O_{TR}$ over the duration of our tree ring records, although other factors may be important at longer time scales. For example, occasional very depleted $\delta^{18}O_P$ values have been reported from rain events in the wet season at eastern coastal sites [*Matsui et al.*, 1983; *Salati et al.*, 1979], thought to be caused by a southward shift of the Intertropical Convergence Zone (ITCZ) reducing the initial isotope value of incoming moisture. In a review of South American monsoon history inferred from stable isotopes, *Vuille et al.* [2012] suggest that latitudinal shifts in the ITCZ may be influential at the scale of several decades to centuries. In addition, sea surface temperature anomalies in the Pacific and Atlantic Oceans are well known to affect Amazon climate [*Marengo and Espinoza*, 2015; *Richey et al.*, 1989; *Yoon and Zeng*, 2010], and are therefore likely to influence $\delta^{18}O_{TR}$ indirectly, by causing more or less precipitation and driving changes in circulation [*Thompson et al.*, 2013; *Vuille et al.*, 2003]. Longer $\delta^{18}O_{TR}$ records than that presented in this paper could possibly shed more light on these decadal-scale influences.

5. Summary

Trajectory modeling and large-scale water vapor transport analysis have been used to identify climatic controls on interannual variation in $\delta^{18}O_{TR}$. The most important single control on $\delta^{18}O_{TR}$ is rainout during moisture transport over the Amazon basin. Interannual variation in atmospheric circulation is another important influence, providing further evidence that within-basin processes regulate $\delta^{18}O_{TR}$. These results provide a mechanistic link to explain why a $\delta^{18}O_{TR}$ chronology from a single site at the end of the basin can be good proxy for precipitation over the entire Amazon region, with wider implications for the interpretation of other paleoproxies in the Amazon.

References

Anchukaitis, K. J., and M. N. Evans (2010), Tropical cloud forest climate variability and the demise of the Monteverde golden toad, *Proc. Natl. Acad. Sci. U.S.A.*, *107*(11), 5036–5040.

Andreae, M., D. Rosenfeld, P. Artaxo, A. Costa, G. Frank, K. Longo, and M. Silva-Dias (2004), Smoking rain clouds over the Amazon, *Science*, *303*(5662), 1337–1342.

Baker, J. C., et al. (2015), Oxygen isotopes in tree rings show good coherence between species and sites in Bolivia, *Global Planet. Change*, *133*, 298–308.

Ballantyne, A., P. Baker, J. Chambers, R. Villalba, and J. Argollo (2011), Regional differences in South American monsoon precipitation inferred from the growth and isotopic composition of tropical trees, *Earth Interact.*, *15*(5), 1–35, doi:10.1175/2010EI277.1.

Barbour, M. M., J. S. Roden, G. D. Farquhar, and J. R. Ehleringer (2004), Expressing leaf water and cellulose oxygen isotope ratios as enrichment above source water reveals evidence of a Péclet effect, *Oecologia*, *138*(3), 426–435.

Boysen, B. M. M., M. N. Evans, and P. J. Baker (2014), $\delta^{18}O$ in the tropical conifer *Agathis robusta* records ENSO-related precipitation variations, *PLoS One*, *9*(7), 9.

Brienen, R. J. W., and P. A. Zuidema (2005), Relating tree growth to rainfall in Bolivian rain forests: A test for six species using tree ring analysis, *Oecologia*, *146*(1), 1–12.

Brienen, R. J. W., G. Helle, T. L. Pons, J. L. Guyot, and M. Gloor (2012), Oxygen isotopes in tree rings are a good proxy for Amazon precipitation and El Niño–Southern Oscillation variability, *Proc. Natl. Acad. Sci. U.S.A.*, *109*(42), 16,957–16,962.

Brown, D., J. Worden, and D. Noone (2008), Comparison of atmospheric hydrology over convective continental regions using water vapor isotope measurements from space, *J. Geophys. Res.*, *113*, D15124, doi:10.1029/2007JD009676.

Bruijnzeel, L., M. Mulligan, and F. N. Scatena (2011), Hydrometeorology of tropical montane cloud forests: Emerging patterns, *Hydrol. Processes*, *25*(3), 465–498.

Callède, J., J. Ronchail, J.-L. Guyot, and E. D. Oliveira (2008), Déboisement amazonien: Son influence sur le débit de l'Amazone à Óbidos (Brésil), *Revue des sciences de l'eau/J. Water Sci.*, *21*(1), 59–72.

Cernusak, L. A., et al. (2016), Stable isotopes in leaf water of terrestrial plants, *Plant Cell Environ.*, *39*, 1087–1102, doi:10.1111/pce.12703.

Cruz, F. W., S. J. Burns, I. Karmann, W. D. Sharp, M. Vuille, A. O. Cardoso, J. A. Ferrari, P. L. S. Dias, and O. Viana (2005), Insolation-driven changes in atmospheric circulation over the past 116,000 years in subtropical Brazil, *Nature*, *434*(7029), 63–66.

Dansgaard, W. (1964), Stable isotopes in precipitation, *Tellus*, *16*(4), 436–468.

Drumond, A., J. Marengo, T. Ambrizzi, R. Nieto, L. Moreira, and L. Gimeno (2014), The role of the Amazon Basin moisture in the atmospheric branch of the hydrological cycle: A Lagrangian analysis, *Hydrol. Earth Syst. Sci*, *18*, 2577–2598.

Dünisch, O., V. R. Montóia, and J. Bauch (2003), Dendroecological investigations on *Swietenia macrophylla* King and *Cedrela odorata* L.(Meliaceae) in the central Amazon, *Trees*, *17*(3), 244–250.

Espinoza, J. C., J. Ronchail, J. L. Guyot, C. Junquas, P. Vauchel, W. Lavado, G. Drapeau, and R. Pombosa (2011), Climate variability and extreme drought in the upper Solimões River (western Amazon Basin): Understanding the exceptional 2010 drought, *Geophys. Res. Lett.*, *38*, L13406, doi:10.1029/2011GL047862.

Fiorella, R. P., C. J. Poulsen, R. S. Pillco Zolá, J. B. Barnes, C. R. Tabor, and T. A. Ehlers (2015), Spatiotemporal variability of modern precipitation δ^{18}O in the central Andes and implications for paleoclimate and paleoaltimetry estimates, *J. Geophys. Res. Atmos.*, *120*, 4630–4656, doi:10.1002/2014JD022893.

Grootes, P., M. Stuiver, L. Thompson, and E. Mosley-Thompson (1989), Oxygen isotope changes in tropical ice, Quelccaya, Peru, *J. Geophys. Res.*, *94*(D1), 1187–1194, doi:10.1029/JD094iD01p01187.

Henderson-Sellers, A., K. McGuffie, and H. Zhang (2002), Stable isotopes as validation tools for global climate model predictions of the impact of Amazonian deforestation, *J. Clim.*, *15*(18), 2664–2677.

Hoffmann, G. (2003a), Taking the pulse of the tropical water cycle, *Science*, *301*(5634), 776–777.

Hoffmann, G. (2003b), Coherent isotope history of Andean ice cores over the last century, *Geophys. Res. Lett.*, *30*(4, 1179), doi:10.1029/2002GL014870.

Holloway, M. D., L. C. Sime, J. S. Singarayer, J. C. Tindall, and P. J. Valdes (2016), Reconstructing paleosalinity from δ^{18}O: Coupled model simulations of the Last Glacial Maximum, Last Interglacial and late Holocene, *Quat. Sci. Rev.*, *131*, 350–364.

Huffman, G. J. (1997), Estimates of root-mean-square random error for finite samples of estimated precipitation, *J. Appl. Meteorol.*, *36*(9), 1191–1201.

Huffman, G. J., D. T. Bolvin, E. J. Nelkin, D. B. Wolff, R. F. Adler, G. Gu, Y. Hong, K. P. Bowman, and E. F. Stocker (2007), The TRMM Multisatellite Precipitation Analysis (TMPA): Quasi-global, multiyear, combined-sensor precipitation estimates at fine scales, *J. Hydrometeorol.*, *8*(1), 38–55.

Hurley, J., M. Vuille, and D. Hardy (2016), Forward modeling of δ^{18}O in Andean ice cores, *Geophys. Res. Lett.*, *43*, 8178–8188, doi:10.1002/2016GL070150.

Hurley, J., M. Vuille, D. Hardy, S. Burns, and L. G. Thompson (2015), Cold air incursions, δ^{18}O variability, and monsoon dynamics associated with snow days at Quelccaya Ice Cap, Peru, *J. Geophys. Res. Atmos.*, *120*, 7467–7487, doi:10.1002/2015JD023323.

Insel, N., C. J. Poulsen, C. Sturm, and T. A. Ehlers (2013), Climate controls on Andean precipitation δ^{18}O interannual variability, *J. Geophys. Res. Atmos.*, *118*, 9721–9742, doi:10.1002/jgrd.50619.

Kahmen, A., D. Sachse, S. K. Arndt, K. P. Tu, H. Farrington, P. M. Vitousek, and T. E. Dawson (2011), Cellulose δ^{18}O is an index of leaf-to-air vapor pressure difference (VPD) in tropical plants, *Proc. Natl. Acad. Sci. U.S.A.*, *108*(5), 1981–1986.

Kanner, L. C., S. J. Burns, H. Cheng, R. L. Edwards, and M. Vuille (2013), High-resolution variability of the South American summer monsoon over the last seven millennia: Insights from a speleothem record from the central Peruvian Andes, *Quat. Sci. Rev.*, *75*, 1–10.

LeGrande, A. N., and G. A. Schmidt (2006), Global gridded data set of the oxygen isotopic composition in seawater, *Geophys. Res. Lett.*, *33*, L12604, doi:10.1029/2006GL026011.

Majoube, M. (1971), Oxygen-18 and deuterium fractionation between water and steam, *J. de Chimie Physique et de Physico-Chimie Biologique*, *68*(10), 1423–1436.

Marengo, J., and J. Espinoza (2015), Extreme seasonal droughts and floods in Amazonia: Causes, trends and impacts, *Int. J. Climatol.*, *36*, 1033–1050, doi:10.1002/joc.4420.

Marengo, J., J. Tomasella, L. Alves, W. Soares, and D. Rodriguez (2011), The drought of 2010 in the context of historical droughts in the Amazon region, *Geophys. Res. Lett.*, *38*, L12703, doi:10.1029/2011GL047436.

Maslin, M. A., and S. J. Burns (2000), Reconstruction of the Amazon Basin effective moisture availability over the past 14,000 years, *Science*, *290*(5500), 2285–2287.

Matsui, E., E. Salati, M. Ribeiro, C. Ris, A. Tancredi, and J. Gat (1983), Precipitation in the central Amazon Basin: The isotopic composition of rain and atmospheric moisture at Belem and Manaus, *Acta Amazonica*, *13*(2), 307–369, doi:10.1590/1809-43921983132307.

McCarroll, D., and N. J. Loader (2004), Stable isotopes in tree rings, *Quat. Sci. Rev.*, *23*(7-8), 771–801.

Moquet, J., et al. (2016), Calibration of speleothem δ^{18}O records against hydroclimate instrumental records in central Brazil, *Global Planet. Change*, *139*, 151–164.

Myneni, R., S. Hoffman, Y. Knyazikhin, J. Privette, J. Glassy, Y. Tian, Y. Wang, X. Song, Y. Zhang, and G. Smith (2002), Global products of vegetation leaf area and fraction absorbed PAR from year one of MODIS data, *Remote Sens. Environ.*, *83*(1), 214–231.

Pierrehumbert, R. T. (1999), Huascaran δ^{18}O as an indicator of tropical climate during the Last Glacial Maximum, *Geophys. Res. Lett.*, *26*(9), 1345–1348, doi:10.1029/1999GL900183.

Poussart, P. F., M. N. Evans, and D. P. Schrag (2004), Resolving seasonality in tropical trees: Multi-decade, high-resolution oxygen and carbon isotope records from Indonesia and Thailand, *Earth Planet. Sci. Lett.*, *218*(3), 301–316.

Richey, J. E., C. Nobre, and C. Deser (1989), Amazon river discharge and climate variability: 1903 to 1985, *Science*, *246*(4926), 101–103.

Roden, J. S., G. Lin, and J. R. Ehleringer (2000), A mechanistic model for interpretation of hydrogen and oxygen isotope ratios in tree-ring cellulose, *Geochim. Cosmochim. Acta*, *64*(1), 21–35.

Salati, E., A. Dall'Olio, E. Matsui, and J. R. Gat (1979), Recycling of water in the Amazon basin: An isotopic study, *Water Resour. Res.*, *15*(5), 1250–1258, doi:10.1029/WR015i005p01250.

Samanta, A., M. H. Costa, E. L. Nunes, S. A. Vieira, L. Xu, and R. B. Myneni (2011), Comment on "Drought-induced reduction in global terrestrial net primary production from 2000 through 2009", *Science*, *333*, 1093.

Samuels-Crow, K. E., J. Galewsky, D. R. Hardy, Z. D. Sharp, J. Worden, and C. Braun (2014), Upwind convective influences on the isotopic composition of atmospheric water vapor over the tropical Andes, *J. Geophys. Res. Atmos.*, *119*, 7051–7063, doi:10.1002/2014JD021487.

Sano, M., C. Xu, and T. Nakatsuka (2012), A 300-year Vietnam hydroclimate and ENSO variability record reconstructed from tree ring δ^{18}O, *J. Geophys. Res.*, *117*, D12115, doi:10.1029/2012JD017749.

Schollaen, K., C. Karamperidou, P. Krusic, E. Cook, and G. Helle (2014), ENSO flavors in a tree-ring δ^{18}O record of Tectona grandis from Indonesia, *Clim. Past Discuss.*, *10*(5), 3965–3987.

Smith, T. M., P. A. Arkin, J. J. Bates, and G. J. Huffman (2006), Estimating bias of satellite-based precipitation estimates, *J. Hydrometeorol.*, *7*(5), 841–856.

Spracklen, D. V., S. R. Arnold, and C. M. Taylor (2012), Observations of increased tropical rainfall preceded by air passage over forests, *Nature*, *489*(7415), 282–285.

Sternberg, L. d. S. L. (2009), Oxygen stable isotope ratios of tree-ring cellulose: The next phase of understanding, *New Phytol.*, *181*(3), 553–562.

Sternberg, L. d. S. L., and M. J. DeNiro (1983), Biogeochemical implications of the isotopic equilibrium fractionation factor between the oxygen atoms of acetone and water, *Geochim. Cosmochim. Acta*, *47*(12), 2271–2274.

Stohl, A. (1998), Computation, accuracy and applications of trajectories—a review and bibliography, *Atmos. Environ.*, *32*(6), 947–966.

Stohl, A., and P. Seibert (1998), Accuracy of trajectories as determined from the conservation of meteorological tracers, *Q. J. R. Meteorol. Soc.*, *124*(549), 1465–1484.

Sturm, C., G. Hoffmann, and B. Langmann (2007), Simulation of the stable water isotopes in precipitation over South America: Comparing regional to global circulation models, *J. Clim.*, *20*(15), 3730–3750.

Thompson, L. G., E. Mosley-Thompson, and M. E. Davis (1995), Late glacial stage and Holocene tropical ice core records from Huascaran, Peru, *Science*, *269*(5220), 46–50, doi:10.1126/science.269.5220.46.

Thompson, L. G., E. Mosley-Thompson, and K. A. Henderson (2000), Ice-core palaeoclimate records in tropical South America since the Last Glacial Maximum, *J. Quat. Sci.*, *15*(4), 377–394.

Thompson, L. G., E. Mosley-Thompson, H. Brecher, M. Davis, B. León, D. Les, P.-N. Lin, T. Mashiotta, and K. Mountain (2006), Abrupt tropical climate change: Past and present, *Proc. Natl. Acad. Sci. U.S.A.*, *103*(28), 10,536–10,543.

Thompson, L. G., E. Mosley-Thompson, M. E. Davis, V. S. Zagorodnov, I. M. Howat, V. N. Mikhalenko, and P. N. Lin (2013), Annually resolved ice core records of tropical climate variability over the past ~1800 years, *Science*, *340*(6135), 945–950.

van der Ent, R. J., H. H. Savenije, B. Schaefli, and S. C. Steele-Dunne (2010), Origin and fate of atmospheric moisture over continents, *Water Resour. Res.*, *46*(9), doi:10.1029/2010WR009127.

Villacís, M., F. Vimeux, and J. D. Taupin (2008), Analysis of the climate controls on the isotopic composition of precipitation (δ^{18}O) at Nuevo Rocafuerte, 74.5°W, 0.9°S, 250 m, Ecuador, *C. R. Geosci.*, *340*(1), 1–9.

Vimeux, F., R. Gallaire, S. Bony, G. Hoffmann, and J. C. Chiang (2005), What are the climate controls on δD in precipitation in the Zongo Valley (Bolivia)? Implications for the Illimani ice core interpretation, *Earth Planet. Sci. Lett.*, *240*(2), 205–220.

Volland, F., D. Pucha, and A. Braeuning (2016), Hydro-climatic variability in southern Ecuador reflected by tree-ring oxygen isotopes, *Erdkunde*, *70*(1), 69–82.

Vuille, M., R. S. Bradley, M. Werner, R. Healy, and F. Keimig (2003), Modeling δ^{18}O in precipitation over the tropical Americas: 1. Interannual variability and climatic controls, *J. Geophys. Res.*, *108*(D6), doi:10.1029/2001JD002038.

Vuille, M., S. Burns, B. Taylor, F. Cruz, B. Bird, M. Abbott, L. Kanner, H. Cheng, and V. Novello (2012), A review of the South American monsoon history as recorded in stable isotopic proxies over the past two millennia, *Clim. Past*, *8*(4), 1309–1321.

Xu, C., M. Sano, and T. Nakatsuka (2011), Tree ring cellulose δ^{18}O of Fokienia hodginsii in northern Laos: A promising proxy to reconstruct ENSO?, *J. Geophys. Res.*, *116*, D24109, doi:10.1029/2011JD016694.

Xu, C., M. Sano, and T. Nakatsuka (2013), A 400-year record of hydroclimate variability and local ENSO history in northern Southeast Asia inferred from tree-ring delta O-18, *Paleogeogr. Paleoclimatol. Paleoecol.*, *386*, 588–598.

Xu, C., N. Pumijumnong, T. Nakatsuka, M. Sano, and Z. Li (2015), A tree-ring cellulose δ^{18}O-based July–October precipitation reconstruction since AD 1828, northwest Thailand, *J. Hydrol.*, *529*, 433–441.

Yan, K., T. Park, G. Yan, C. Chen, B. Yang, Z. Liu, R. R. Nemani, Y. Knyazikhin, and R. B. Myneni (2016), Evaluation of MODIS LAI/FPAR product collection 6. Part 1: Consistency and improvements, *Remote Sens.*, *8*(5), 359.

Yoon, J.-H., and N. Zeng (2010), An Atlantic influence on Amazon rainfall, *Clim. Dyn.*, *34*(2–3), 249–264.